Journal of Multidisciplinary Engineering Science and Technology (JMEST)
ISSN: 2458-9403
Vol. 4 Issue 8, August - 2017

Self-Energy And Energy Loss Of Charge Particle Channeling In Carbon Nanotubes

***Bahaa H. Abbass ** Khalid A. Ahmad ** Riyahd K. Ahmed**
**Al-Mustansiriyah University, College of Science, Department of Physics.
Baghdad-Iraq
baha565@yahoo.com
baha565b@gmail.com

***Abstract*—By developing a semiclassical kinetic model to simulate the plasmon excitation of carbon nanotubes and the transport of charged particles moving through nanotubes. The analytical expressions of the dielectric function and the energy loss function are obtained for zigzag and armchair nanotubes of metallic properties, respectively. Numerical results display several very distinct peaks in the curves of loss function, showing effects from the collective excitation. As well, the stopping power and self-energy are calculated while charged particles move along the axis of nanotubes with different geometries, under the influence of friction coefficients. The results had been achieved by using the programs are written in FORTRAN 90 using software Computer Visual FORTRANV6.6, which performed for the numerical calculation, showing the influence of the damping factor, the nanotube radius, and the particle position on its self-energy, loss function and the stopping power.**

Keywords—carbon nanotube, stopping power, self-energy

I. INTRODUCTION

When the carbon nanotube was discovered, there has been a growing interest in interactions of charged particles with the nanotubes, which has many applications in fields of research and technology. For example, important information about the electronic structure of carbon nanotubes can be obtained using the electron probe techniques, such as the transmission-electron microscopy [1] and the electron energy-loss spectroscopy (EELS) [2,3]. In particular, in some of the most intriguing applications, it has been demonstrated that carbon nanotubes may be used to efficiently directing (deflect and focus) charged particle beams [4,5], in the way quite similar to crystal channeling. A powerful theoretical tool for studying such interactions is provided by the dielectric response formalism, which has been implemented in restricted geometries in a number of pioneering studies by Ritchie and co-workers [6]. Important contribution in that direction has been reported by Stöckli *et al.*[7], who have described the dielectric properties of carbon nanotubes by means of the hydrodynamic theory of plasmon excitations in a 2D electron gas on a cylindrical surface, in order to interpret the EELS data for collective excitations on single-wall carbon nanotubes, caused by the incidence of fast electrons perpendicular to the nanotube. Given the properties of the hydrodynamic model, such a study is suitable for describing the high-energy electrons passing through, or close by, the carbon nanotubes. On the other hand, experimental study of transport, or channeling, of charged particles through carbon nanotubes in the paraxial direction seems feasible, at present, only in the systems of the so-called ‘‘ropes,’’ or bunches, of nanotubes [8]. In such systems, the interactions of charged particles with the medium may be described, in a first approximation, by the model of a cylindrical cavity in the bulk of a solid [9-11]. Carbon nanotubes present systems that are quite different from the cavities in solids or nanowires made of different materials. Although all these systems share the same underlying cylindrical geometry, carbon nanotubes cannot be modeled as a part of a 3D structure. It is well known that, in general, the dielectric functions of nanotubes exhibit rather rich and complex properties regarding the dependence on the longitudinal wave number, the frequency, and the angular momentum of the elementary excitations, in ways that are strongly influenced by the geometric structure of the nanotube, such as its radius and the chiral angle [12-15].The dielectric formalism [16] used to study the energy loss of charged particles moving parallel to the axis in cylindrical tubules. In that formalism, the elementary excitations of the electron gas are described by dielectric function in the random-phase approximation (RPA) [17].

II. THEORETICAL REVIEW

Zigzag nanotubes ***(n, l=0)*** and armchair nanotubes ***(n, l=n)*** are regarded as infinitesimally thin and infinitely long cylindrical cavities. The ***(n, l)*** nanotube naming scheme can be thought of as a vector in an infinite graphene sheet that describes how to roll up the graphene sheet to make the nanotube. The radius $\boldsymbol{a}$ of a nanotube is connected to $\boldsymbol{l}$ and $\boldsymbol{n}$ in the form of $\boldsymbol{a} = \frac{b\sqrt{3(l^2+ln+n^2)}}{2\pi}$, where (**b=1.44** $\boldsymbol{A^0}$) is the length of the **C-C** bond of the surface of the nanotube. The electrons of the nanotube surface are assumed to meet the Fermi equilibrium distribution function, with the chemical potential of graphite being null valued [16]

$$f_0(p) = \frac{1}{1+\exp\left\{\frac{\varepsilon(p)}{k_B T}\right\}} \qquad (1)$$

where $\boldsymbol{\varepsilon} = \boldsymbol{\varepsilon}(\boldsymbol{p})$ is the electron energy with respect to Fermi level, k_B is the Boltzmann constant, $\boldsymbol{T}$ is the temperature which remains at **273 K** here, and **p** is the electron's two dimensional quasimomentum tangential to the nanotube's surface. In this Work, taken $\boldsymbol{\pi}$ electrons as the aim for their important effects on electronic properties. By using the tight-binding model, the energy dispersion relations for zigzag and armchair nanotubes can be given as [18-20] only

m=0 can be relied on, and the term of $v_{\emptyset}$ would be ignored,

for zigzag (*n*,0) :

$$\varepsilon(p) = \pm\gamma_0\sqrt{1+4\cos\left(\frac{3bp_z}{2\hbar}\right)\cos\left(\frac{\sqrt{3}bp_\phi}{2\hbar}\right)+4\cos^2\left(\frac{\sqrt{3}bp_\phi}{2\hbar}\right)} \quad (2)$$

and **for armchair (*n*, *n*) :**

$$\varepsilon(p) = \pm\gamma_0\sqrt{1+4\cos\left(\frac{3bp_\phi}{2\hbar}\right)\cos\left(\frac{\sqrt{3}bp_z}{2\hbar}\right)+4\cos^2\left(\frac{\sqrt{3}bp_z}{2\hbar}\right)} \quad (3)$$

where p_z and p_ϕ are the projections of **p** on the axis and the ϕ direction of the nanotube,(γ_0 =3.033 eV) is the interaction energy for the nearest-neighbor carbon atoms. The sign $\pm$ corresponds to the conduction and valence electrons, respectively. Different from the graphene plane, carbon nanotubes have a structure with a long fiber axis and a circumference of atomic dimensions. So, while the number of allowed states in the axial direction is large, the number of states in the circumferential direction is limited, resulting in the discrete values of the momentump_ϕ. Using the periodic boundary condition, the allowed values for $p_\phi$can be written for **zigzag (*n*, 0) :**

$$p_\phi = \frac{2\pi\hbar s}{\sqrt{3}nb},\ \text{s=1,2,… ,}n \quad (4)$$

for **armchair (*n*, *n*) :**

$$p_\phi = \frac{2\pi\hbar s}{3nb},\ \text{s=1,2,… ,}n \quad (5)$$

The dielectric function of the electron gas $\epsilon(k,m,\omega,a)$ on the nanotube surface with the form as:

$$\epsilon(k,m,\omega,a) = 1 - 4\pi a I_m(ka)K_m(ka)\chi(k,m,\omega,a), \quad (6)$$

where $4\pi aI_m(ka)\ K_m(ka)$ is the Fourier transform of the electron-electron Coulomb interaction on the surface of nanotube, and $\chi(k,m,\omega,a)$ is the response function, which has different expressions for zigzag and armchair nanotubes in this model, **for zigzag:**

$$\chi(k,m,\omega,a) = \frac{4}{\pi\hbar}\frac{1}{\sqrt{3}nb}\sum_{s=1}^{n}\int_{-2\pi/3b}^{2\pi/3b} dp_z \frac{\partial f_0}{\partial\varepsilon}\frac{\left(\frac{m}{a}\right)v_\phi + kv_z}{\left(\frac{m}{a}\right)v_\phi + kv_z - \omega - i\gamma}, \quad (7)$$

for armchair:

$$\chi(k,m,\omega,a) = \frac{4}{\pi\hbar}\frac{1}{3nb}\sum_{s=1}^{n}\int_{-2\pi/\sqrt{3}b}^{2\pi/\sqrt{3}b} dp_z \frac{\partial f_0}{\partial\varepsilon}\frac{\left(\frac{m}{a}\right)v_\phi + kv_z}{\left(\frac{m}{a}\right)v_\phi + kv_z - \omega - i\gamma}, \quad (8)$$

So, the dielectric function obtained here is not only related to the longitudinal wave number k, the angular momentum m, the frequency ω of the elementary excitation, and the radius of the nanotube, but also the chiral angle of the nanotube which indicates the different energy dispersion relation of electrons in Eqs. (2) and (3).

Considering the asymptotical properties of the modified Bessel function, the term $K_m(k/a)/I_m(k/a)$ in equations of self-energy and stopping power approaches zero at a rapid rate as k increases. Thus more contribution will be made to the stopping power in the case of smaller m and k in this theoretical model.

In the following calculations, a proton Q=1 discussed when it's moving along the axis of the nanotube $\rho_0 = 0$ in zigzag nanotubes and armchair nanotubes, respectively.Thus, on account of axial symmetry, in the expression of the response function. [21].

It is convenient to consider separately the values of the total potential $\varphi = \varphi_1$inside the nanotube ($\rho < a$)and $\varphi = \varphi_2$ outside the nanotube ($\rho > a$). The former part of the potential is composed of the potential $\varphi_0$due to the moving charged particle and the induced potential φ_{ind} due to the charge polarization on the nanotube surface, so that $\varphi_1 = \varphi_0 + \varphi_{ind}$. Taking into account the natural boundary conditions at $\rho = 0$ and $\rho = \infty$, the potential φ_{ind} can be expanded in terms of the cylindrical Bessel functions term $K_m(x)/I_m(x)$, [11, 16] as follows:

$$\varphi_{\text{ind}}(r,t) = \frac{Q}{\pi}\sum_{m=-\infty}^{\infty}\int_{-\infty}^{+\infty} dk e^{ik(z-vt)+\text{im}(\emptyset-\emptyset_0)} I_m(k\,\rho_0)I_m(k\rho)\frac{K_m(ka)}{I_m(ka)}[\epsilon^{-1}(k,m,\omega,a) - 1], \quad (9)$$

So, the detailed expressions of the self-energy and stopping power are given as

$$E_{self} = \frac{1}{2}Q\varphi_{ind}(r,t)|_{r=r_0(t)} = \frac{Q^2}{2\pi}\sum_{-m=\infty}^{m=\infty}\int_{-\infty}^{\infty} dk I_m^2(|k|\rho_0)\frac{K_m(|k|a)}{I_m(|k|a)} \times \{Re\,[\epsilon^{-1}(k,m,\omega,a) - 1]\}, \quad (10)$$

$$S = Q\frac{\partial\varphi_{ind}(r,t)}{\partial z}|_{r=r_0(t)} = \frac{Q^2}{2\pi}\sum_{-m=\infty}^{m=\infty}\int_{-\infty}^{\infty} dk I_m^2(|k|\rho_0)\frac{K_m(|k|a)}{I_m(|k|a)} \times Im\,[\epsilon^{-1}(k,m,\omega,a) - 1], \quad (11)$$

From **Eq. (11)** one may notice that the resonant excitations could be figured out in the case that the damping coefficient approaches zero $\gamma \to 0^+$.

As the function $Z_m(k,\omega) = 4\pi aI_m(ka)K_m(ka)Re\,\chi(k,m,\omega,a)$ equal zero, the energy loss function $[-\epsilon^{-1}(k,m,\omega,a)]$ in Eq. (10) transforms into a Delta function, leading to

$$S = \frac{Q^2}{2\pi}\sum_{-m=\infty}^{m=\infty}\int_{-\infty}^{\infty} k_m I_m^2(|k_m|\rho_0)\frac{K_m(|k|a)}{I_m(|k|a)}\frac{\partial Z_m(k,\omega)}{\partial k}|_{k=k_m}^{-1}, \quad (12)$$

Where:

k_m is determined by the condition of the collective resonance $Z_m(k,\omega) = 0$

III RESULTS

The dielectric functions $\varepsilon(k, m, \omega, a)$ vs the frequency ω for zigzag nanotube **(27, 0)** and armchair nanotube **(15, 15)** are shown in Figures **(1)**, with γ/ω_p=0.001, m = 0 and $\omega_p = (\frac{4\pi n_0}{a})^{1/2}$= 0.5 a.u., n_0 is the surface density of the valence electrons, which is obtained from the integration of equilibrium distribution functions $n_0 = \frac{4}{(4\pi\hbar)^2}\int \mathbf{dpf_0}(\mathbf{a}, \mathbf{p})$, [22].

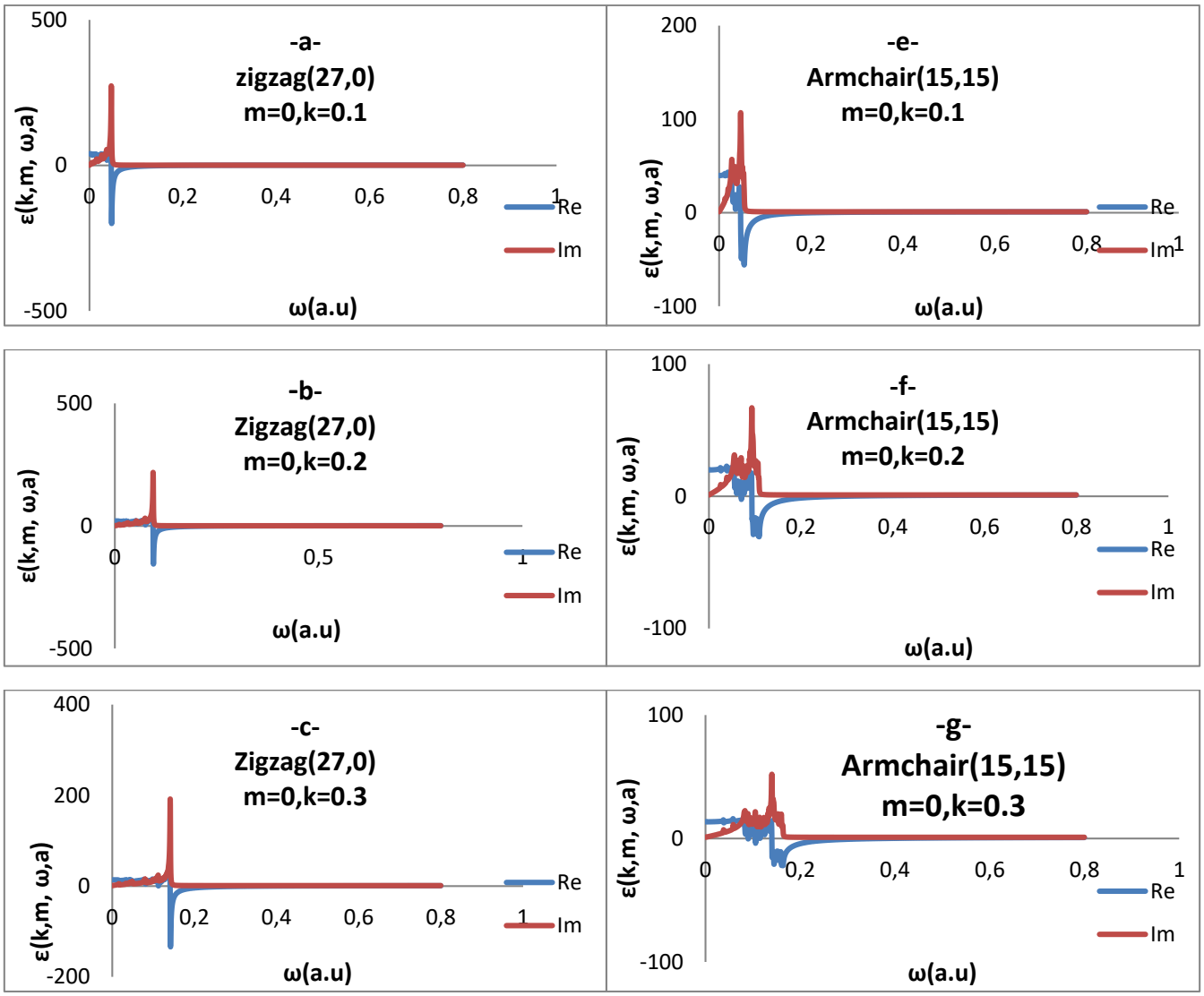

FIG.1. The dielectric functions dependent on the frequency ω for zigzag (27, 0) carbon nanotubes are shown in (a, b, c) and armchair (15, 15) carbon nanotubes are shown in (e, f, g) , with m =0, γ/ω_p=0.001 and different k=0.1, 0.2, and 0.3. The real (Re) and the imaginary (Im) of the dielectric function is shown by the blue and the red curves, respectively.

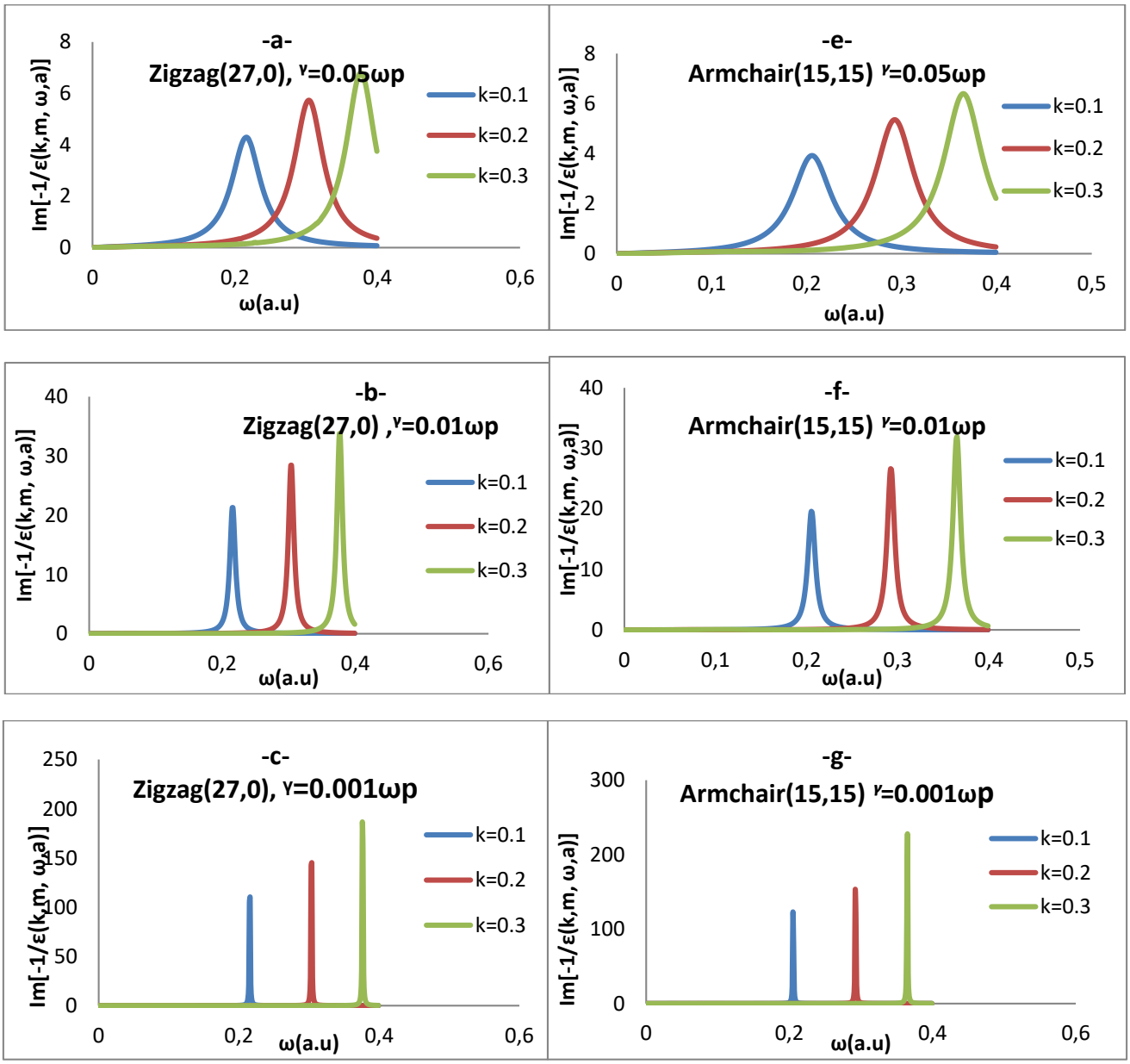

FIG.2.The loss functions dependent on the frequency, ω for zigzag (27, 0) carbon nanotubes are shown in (a, b, c) and armchair (15, 15) carbon nanotubes are shown in (e, f, g), with *m*=0, and different *k* and values γ.

The real part **Re** and the imaginary part ***Im*** of the dielectric function are shown by the blue and the red curves, respectively. One can see from this figure that the curves of ***Re*** and ***Im*** exhibit similar shapes. Which the theoretical formulation is based on the quantum RPA. Obviously, as the arrows point out in **Fig.1**, the trend of ***Re*** is becoming zero with the increasing of **ω**, while ***Im*** approaches zero with the infinitesimally small damping, corresponding to collective excitations on the nanotube surface.

Plasmon peaks are also shown in **Fig.1**, in which the energy loss function small damping, corresponding to collective excitations on the nanotube surface. $\mathbf{Im}[\boldsymbol{\varepsilon}^{-1}(\boldsymbol{k},\boldsymbol{m},\boldsymbol{\omega},\boldsymbol{a})]$ is calculated dependent on the frequency **ω** but for different damping $\boldsymbol{\gamma}$. The biggest damping factor adopted here is $\boldsymbol{\gamma} = \mathbf{0.05}\ \boldsymbol{\omega_p} \approx \mathbf{0.68\ eV}$.
It can be observed that the plasmon peaks are damped to become lower and wider for more friction from the atoms.

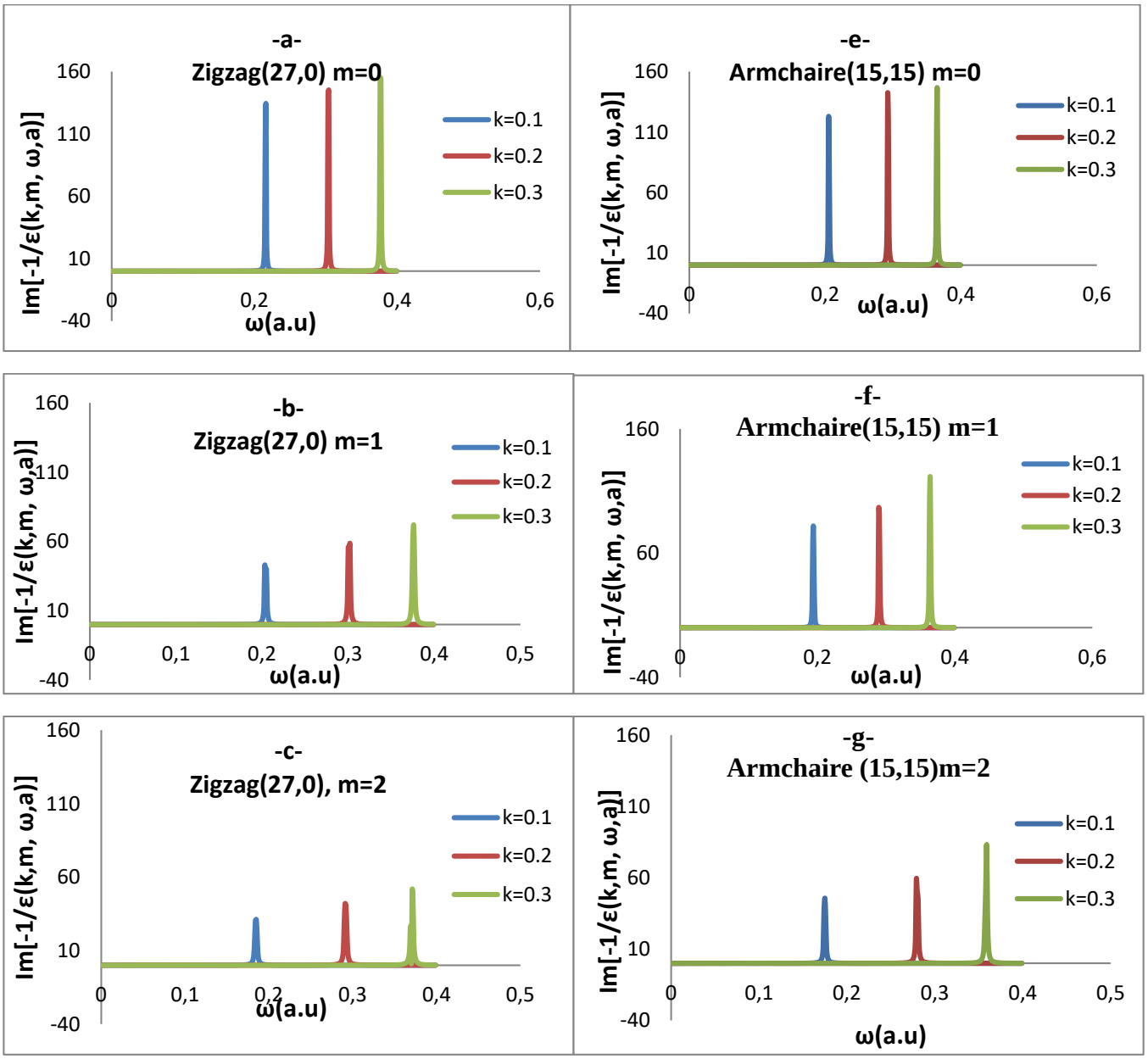

FIG.3. The loss functions dependent on the frequency ω for a zigzag (27, 0)carbon nanotubes are shown in (a, b, c) and for a armchair (15, 15) carbon nanotubes are shown in (e, f, g), with γ/ω_p=0.001, and different *k* and *m* values.

The angular momentum ***m*=0, 1**, and **2**. As ***m*** decreases and ***k*** increases, the peak value keeps increasing, suggesting more energy loss.

However, considering the asymptotical properties of the modified Bessel function, the term $\boldsymbol{K_m}(\boldsymbol{k}/\boldsymbol{a})/\boldsymbol{I_m}(\boldsymbol{k}/\boldsymbol{a})$ in equations of self-energy and stopping power approaches zero at a rapid rate as ***k*** increases. Thus more contribution will be made to the stopping power in the case of smaller ***m*** and ***k*** in this theoretical model.

In the following calculations, a proton ***Q*=1** discussed when it's moving along the axis of the nanotube $\boldsymbol{\rho_0 = 0}$ in zigzag nanotubes and armchair nanotubes, respectively. Thus, on account of axial symmetry, only *m*=0 can be relied on, and the term of $\boldsymbol{v_\emptyset}$ would be ignored in the expression of the response function. **[21]**

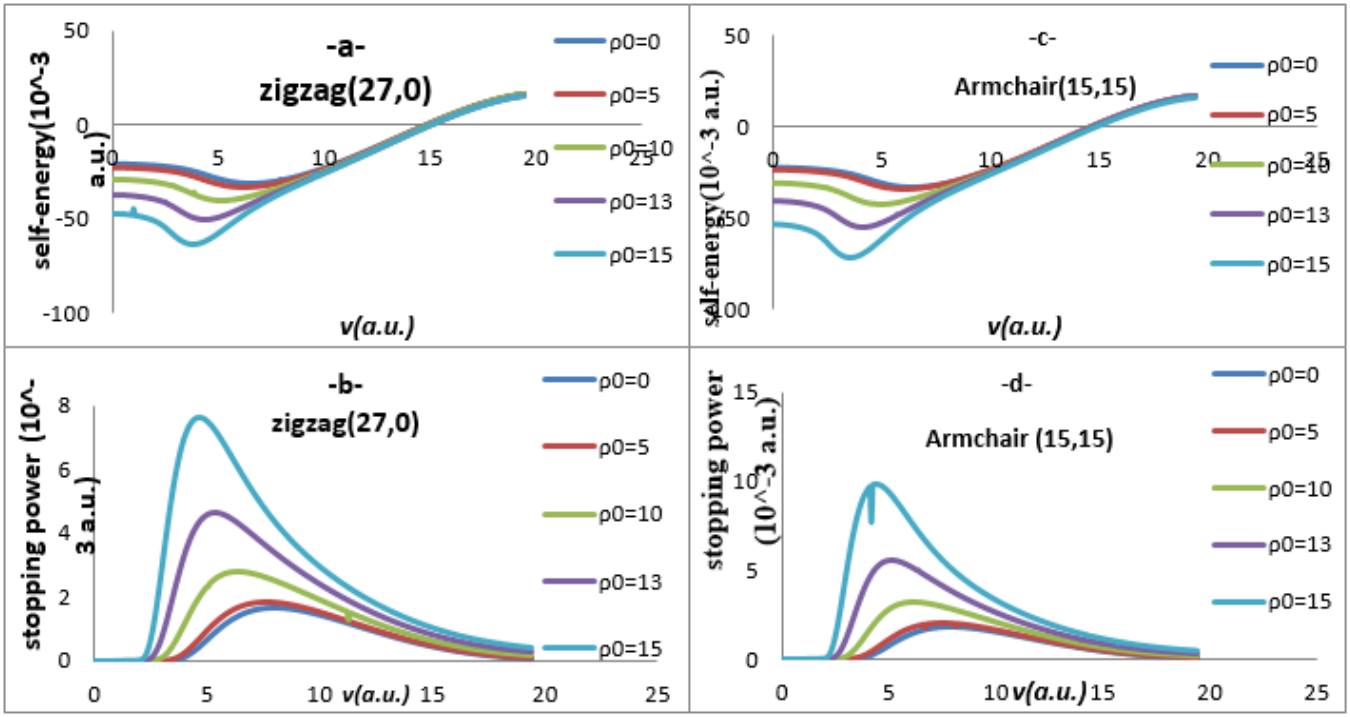

FIG.4. Effects of the particle position ρ_0 on the velocity dependence of the self-energy with γ/ω_p=0.001 are shown in(a)and (c), for a proton moving in zigzag (27, 0) and carbon nanotubes and armchair (15, 15) carbon nanotube, respectively.(b)and (d) shown the stopping power with friction coefficient (γ=0), for a proton moving in zigzag (27, 0) carbon nanotubes and armchair (15, 15) carbon nanotube, respectively.

The influence of the charged particle position $\boldsymbol{\rho_0}$ on the dependence of the self-energy and the energy loss on velocity are shown in Figs. (**4**), for $\boldsymbol{a}$=**20** and with zero friction coefficient (γ=**0**).

For a fixed velocity, both the self-energy and the stopping power have the smallest magnitude when the particle moves along the nanotube axis, and increase in magnitude when the particle position shifts closer to the surface of the nanotube. One also observes that the positions of extreme a in both sets of curves shift to lower velocities as the particle position moves closer to the wall of the nanotube.

IV Conclusion

In this work, a theoretical calculation is used to describe the electron excitation on the surface of the zigzag and armchair nanotubes of metallic character. From the electron dispersion relation of the nanotube, the real band structure of electrons can be embodied to affect the characters of the dielectric function $\boldsymbol{\epsilon(k,m,\omega,a)}$ and the loss function **Im[** $\boldsymbol{-\epsilon^{-1}(k,m,\omega,a)}$**]** . General expressions of the dielectric function and energy loss function are accordingly derived, which are relative to the radius and chiral angle of the nanotubes. The plasmon excitation, which is dependent on the nanotube geometry, the longitudinal wave number, the angular momentum, and the friction coefficient, can be identified from the dielectric function profiles and the sharp peaks in the loss function. And then, the self-energy, and the stopping power are obtained for a charged particle moving paraxially in nanotubes. The simulation results are shown and indicate strong dependences on the damping factor and the nanotube geometry. As the damping factor $\boldsymbol{\gamma}$ increases, the self-energy and the stopping power keep decreasing in magnitude, and the extrema position of the stopping power move to the lower velocity region, suggesting more damping effects on the collective excitation. The stopping power results also show that the damping $\boldsymbol{\gamma = 0.001\omega_p}$ is small enough to be taken as a case without damping. And in this case, as the radius of the two kinds of nanotube increases, the self-energy and the stopping power decrease in magnitude, but with almost no shifts of the maxima position. [16]. The results obtained make researchers believe that the present model is available and apt for studies of the transport behavior through nanotubes, especially for different nanotube geometries and even for multiwall nanotubes in future work.

References

[1] A. Rivacoba, P. Appell, and N. Zabala, Nucl. Instrum. Methods Phys. Res. B **96**, 465 (1995).

[2] T. Pichler, M. Knupfer, M.S. Golden, and J. Fink, Phys. Rev.Lett. **80**,47291(1998)

[3] M. Knupfer *et al.*, Carbon **37**, 733 (1999).

[4] N.K. Zhevago and V.I. Glebov, Phys. Lett. A **310**, 301 (2003).

[5] L.A. Gevorgian, K.A. Ispirian, and R.K. Ispirian, Nucl. Instrum. Methods Phys. Res. B **145**, 155 (1998).

[6] D.P. Spears, J.D. Allen, V.E. Anderson, R.S. Becker, H.H. Hubbell, T.L. Ferrel, R.H. Ritchie, and R.D. Birkhoff, J. Appl. Phys. **50**, 3039 (1979); R.S. Becker,V.E.Anderson, R.D. Birkhoff, T.L. Ferrel, and R.H. Ritchie, Can. J. Phys. **59**, 521 (1981).

[7] T. Sto¨ckli, J.M. Bonard, A. Chaˆtelain, Z.L. Wang, and P. Stadelmann,Phys. Rev. B **64**, 115424 (2001).

[8] L.A. Gevorgian, K.A. Ispirian, and R.K. Ispirian, Nucl. Instrum. Methods Phys. Res. B **145**, 155(1998).**[9]** N.R. Arista and M.A. Fuentes, Phys. Rev. B **63**, 165401 (2001).

[10] N.R. Arista, Phys. Rev. A **64**, 032901 (2001).

[11] N.R. Arista, Nucl. Instrum. Methods Phys. Res. B **182**, 109 (2001).

[12] O. Sato, Y. Tanaka, M. Kobayshi, and A. Hasegawa, Phys. Rev. B **48**, 1947 (1993).
[13] M.F. Lin and Kenneth W.K. Shung, Phys. Rev. B **47**, 6617 (1993).
[14] M.F. Lin, D.S. Chun, C.S. Huang, and Y.K. Lin, Phys. Rev. B **53**, 15 493(1996).
[15] M.F. Lin and F.L. Shyu, Physica B **292**, 117 (2000).
[16] Y.N. Wang and Z.L. Misˇkovic´, Phys. Rev. A **66**, 042904 (2002).

[17] M.F. Lin and K.W.-K. Shung, Phys. Rev. B **47**, 6617 (1993).

[18] G. Ya. Slepyan, S. A. Maksimenko, A. Lakhtakia, O. Yevtushenko, and A. V. Gusakov, Phys. Rev. B **60**, 17136 (1999)]

[19] R. Saito, M. Fujita, G. Dresselhaus, and M. S. Dresselhaus, Phys. Rev. B **46**, 1804 (1992).

[20] M. F. Lin and W.-K. Kenneth Shung, Phys. Rev. B **52**, 8423(1995)

[21] D. Ostling, D. Tomanek, and A. Rosen, Phys. Rev. B **55**, 13 980 (1997).

[22] Y.H. Song, Z.D., and Y.N. Wang Phy. Rev.A**78**,012901(2008).